

UCSF

UC San Francisco Previously Published Works

Title

A20 and ABIN-1 synergistically preserve intestinal epithelial cell survival.

Permalink

<https://escholarship.org/uc/item/0ct018p5>

Journal

The Journal of experimental medicine, 215(7)

ISSN

0022-1007

Authors

Kattah, Michael G
Shao, Ling
Rosli, Yenny Y
[et al.](#)

Publication Date

2018-07-01




DOI

10.1084/jem.20180198

Peer reviewed

ARTICLE

A20 and ABIN-1 synergistically preserve intestinal epithelial cell survival

Michael G. Kattah*, Ling Shao* , Yenny Y. Rosli, Hiromichi Shimizu, Michael I. Whang, Rommel Advincula, Philip Achacoso, Sanjana Shah, Bao H. Duong, Michio Onizawa, Priscilia Tanbun, Barbara A. Malynn , and Averil Ma 

A20 (*TNFAIP3*) and ABIN-1 (*TNIP1*) are candidate susceptibility genes for inflammatory bowel disease and other autoimmune or inflammatory diseases, but it is unclear how these proteins interact in vivo to prevent disease. Here we show that intestinal epithelial cell (IEC)-specific deletion of either A20 or ABIN-1 alone leads to negligible IEC loss, whereas simultaneous deletion of both A20 and ABIN-1 leads to rapid IEC death and mouse lethality. Deletion of both A20 and ABIN-1 from enteroids causes spontaneous cell death in the absence of microbes or hematopoietic cells. Studies with enteroids reveal that A20 and ABIN-1 synergistically restrict death by inhibiting TNF-induced caspase 8 activation and RIPK1 kinase activity. Inhibition of RIPK1 kinase activity alone, or caspase inhibition combined with RIPK3 deletion, abrogates IEC death by blocking both apoptosis and necroptosis in A20 and ABIN-1 double-deficient cells. These data show that the disease susceptibility proteins A20 and ABIN-1 synergistically prevent intestinal inflammation by restricting IEC death and preserving tissue integrity.

Introduction

Crohn's disease and ulcerative colitis, the two primary forms of inflammatory bowel disease (IBD), are characterized by intestinal inflammation and epithelial cell loss (Hooper, 2015; Wlodarska et al., 2015). Genome-wide association studies (GWAS) have identified hundreds of risk alleles for IBD, but it is unclear how multiple alleles with small individual effects conspire to cause profound disease in individual patients (Jostins et al., 2012; Ma and Malynn, 2012; Wang et al., 2013; Catrysse et al., 2014). Dissecting epistatic genetic interactions is therefore critical to understanding the pathogenesis of multigenic disorders such as IBD. Because disruption of the intestinal epithelium is the histological hallmark of IBD, understanding the gene products that cooperate to preserve intestinal epithelial integrity could lead to new therapies for patients with IBD.

Germline polymorphisms in A20 (*TNFAIP3*) and its binding partner ABIN-1 (*TNIP-1*) are correlated with the incidence and severity of multiple inflammatory and autoimmune diseases, including IBD, psoriasis, rheumatoid arthritis, systemic lupus erythematosus, and others (Jostins et al., 2012; Ma and Malynn, 2012; Wang et al., 2013; Catrysse et al., 2014; Di Narzo et al., 2016). In addition, reduced expression of A20 in tissues from asthma and IBD patients without germline polymorphisms suggests that epigenetic pathophysiologic factors may also suppress A20

expression (Arnesescu et al., 2008; Bruno et al., 2015; Schuijjs et al., 2015; Majumdar et al., 2017). Furthermore, heterozygous germline mutations of A20 cause reduced A20 expression and monogenic early-onset inflammatory diseases in human patients, characterized by mucosal ulceration (Zhou et al., 2016). These lines of genetic and epigenetic evidence suggest that compromised expression or function of A20 and/or ABIN-1 predispose patients to these diseases. The correlations between reduced A20 and ABIN-1 expression and disease raise the critical question of how these proteins prevent disease.

A20 and ABIN-1 are both ubiquitin interacting proteins that restrict NF- κ B signaling and restrict cell death (Opipari et al., 1990; Heyninck et al., 1999; Lee et al., 2000; Wagner et al., 2008; Oshima et al., 2009; Bosanac et al., 2010; Nanda et al., 2011; Skaug et al., 2011; Tokunaga et al., 2012; Verhelst et al., 2012; Lu et al., 2013; Wertz et al., 2015). A20 and ABIN-1 directly restrict TNF and TLR induced signals (Boone et al., 2004; Wertz et al., 2004). A20 exhibits both ubiquitin-binding and ubiquitin-modifying enzymatic activity (Boone et al., 2004; Wertz et al., 2004), whereas ABIN-1 possesses only ubiquitin-binding activity (Nanda et al., 2011). Because A20 and ABIN-1 are binding partners (Heyninck et al., 1999), and because they function in similar pathways, a prevailing model depicts ABIN-1 functioning as an

Department of Medicine, University of California, San Francisco, San Francisco, CA.

*M.G. Kattah and L. Shao contributed equally to this paper; Correspondence to Averil Ma: averil.ma@ucsf.edu; L. Shao's present address is Dept. of Medicine, University of Southern California, Los Angeles, CA.

© 2018 Kattah et al. This article is distributed under the terms of an Attribution–Noncommercial–Share Alike–No Mirror Sites license for the first six months after the publication date (see <http://www.rupress.org/terms/>). After six months it is available under a Creative Commons License (Attribution–Noncommercial–Share Alike 4.0 International license, as described at <https://creativecommons.org/licenses/by-nc-sa/4.0/>).

adaptor for A20. In this scenario, ABIN-1 would help bring A20 to ubiquitinated signaling complexes where A20 could exert its enzymatic functions (Dziedzic et al., 2018). Loss of either protein could be predicted to lead to similar cellular and physiological defects. However, the epistatic relationship between these biochemically linked disease susceptibility proteins has not been examined.

Although most previous studies of A20 and ABIN-1 functions *in vivo* have highlighted the importance of these proteins in regulating immune cell activation (Lee et al., 2000; Tavares et al., 2010; Nanda et al., 2011; Ma and Malynn, 2012; Callahan et al., 2013; Catrysse et al., 2014; Verstrepen et al., 2014; Wertz and Dixit, 2014; G'Sell et al., 2015; Das et al., 2018), A20 and ABIN-1 are expressed in virtually all cell types, including nonhematopoietic cells such as epithelial cells, endothelial cells, and fibroblasts. Mice with A20-deficient intestinal epithelial cells (IECs) have been previously reported to be grossly normal, although they are more susceptible to inducible intestinal injury with dextran sodium sulfate or intraperitoneal TNF injection and to cancer induced by A20-deficient myeloid cells or collaborating oncogenes (Vereecke et al., 2010, 2014; Shao et al., 2013). The *in vivo* functions of ABIN-1 in IECs have not been studied. In addition, the epistatic relationship between A20 and ABIN-1 has never been addressed. Given the importance of IEC homeostasis to IBD pathophysiology, we have investigated the combinatorial functions of A20 and ABIN-1 in IECs.

Results

Acute deletion of both A20 and ABIN-1 in IECs leads to severe spontaneous enterocolitis

To assess the epistatic relationship between A20 and ABIN-1 *in vivo*, we interbred floxed A20 (A20^{FL}; Tavares et al., 2010) and floxed ABIN-1 (ABIN-1^{FL}; Oshima et al., 2009) mice with villin-ER/Cre mice (el Marjou et al., 2004). The resulting compound-mutant mice allowed inducible deletion of A20 alone, ABIN-1 alone, or both A20 and ABIN-1 selectively in IECs, thereby avoiding potential caveats associated with developmental adaptations or commensal dysbiosis. Unperturbed A20^{FL/FL} villin-ER/Cre⁺ mice and ABIN-1^{FL/FL} villin-ER/Cre⁺ mice retained expression of A20 and ABIN-1 and were both grossly normal (unpublished data). Daily injection of tamoxifen into these mice caused significant loss of A20 and/or ABIN-1 proteins from IECs within 40 h after the first injection (Fig. 1A). Acute deletion of A20 alone or ABIN-1 alone from IECs caused no change in mouse survival (Fig. 1B). In marked contrast, deletion of both copies of A20 and ABIN-1 from IECs in A20^{FL/FL}ABIN-1^{FL/FL} villin-ER/Cre⁺ mice led to 100% mortality within 3–5 d (Fig. 1B, red line). Mice lacking both copies of A20 and one copy of ABIN-1 (A20^{FL/FL} ABIN-1^{FL/+} villin-ER/Cre⁺) died with delayed kinetics, between 11 and 14 d (Fig. 1B, blue line). Interestingly, deletion of one copy of A20 and two copies of ABIN-1 in IECs (A20^{FL/+}ABIN-1^{FL/FL} villin-ER/Cre⁺) led to no significant spontaneous pathology (Fig. 1B and data not depicted).

Histologically, mice lacking A20 and ABIN-1 in the intestinal epithelium exhibited profound IEC loss, inflammatory infiltrate,

cryptitis, and loss of mucosal architecture in both the small intestine and colon (Fig. 1, C and D). IEC loss was further characterized by massive apoptotic cell death, as revealed by terminal deoxynucleotidyl transferase dUTP nick-end labeling (TUNEL) staining (Fig. 1, E and F), and cleaved caspase 3 (CC3) immunofluorescence (Fig. 1, G and H). Therefore, ABIN-1 preserves the survival of A20-deficient IECs *in vivo* by restricting apoptotic cell death in a dose-dependent fashion.

The findings above reveal several unexpected insights. First, the dramatic phenotype of A20 and ABIN-1 double-deficient mice contrasts sharply with the normal phenotypes of mice lacking A20 or ABIN-1 alone. Hence, ABIN-1 must perform physiologically critical A20-independent functions, rather than acting primarily as an adaptor for A20. The dramatic phenotype of A20^{FL/FL}ABIN-1^{FL/+} villin-ER/Cre⁺ mice suggests that ABIN-1 expression levels in IECs are critical for intestinal homeostasis. In addition, the fact that A20-deficient, ABIN-1 heterozygous (A20^{FL/FL} ABIN-1^{FL/+} villin-ER/Cre⁺) mice die whereas A20 heterozygous, ABIN-1-deficient (A20^{FL/+}ABIN-1^{FL/FL} villin-ER/Cre⁺) mice survive suggests that A20 compensates for ABIN-1 deficiency better than ABIN-1 compensates for A20. Therefore, a synergistic, though asymmetric, relationship exists between these disease susceptibility proteins. Finally, the phenotypes we observed were grossly evident under basal conditions, without overt stressors such as dextran sulfate sodium or pathogenic microbes. Hence, A20 and ABIN-1 perform critical functions in regulating homeostatic signals in unperturbed mice. Taken together, these results reveal a surprisingly potent synergy between A20 and ABIN-1 in preserving IEC survival *in vivo*.

Both TNF-dependent and TNF-independent signals contribute to acute mortality *in vivo*

Anti-TNF agents are the most frequently prescribed biologics for treating IBD (van Deen et al., 2014). Additionally, A20 and ABIN-1 both restrict TNF-induced cell death, and inhibiting death of IECs may be an important mechanism by which anti-TNF treatment restores intestinal homeostasis in patients suffering from IBD (Zeissig et al., 2004). However, TNF deficiency does not prevent inflammation in A20^{-/-} or ABIN-1^{-/-} mice (Lee et al., 2000; Nanda et al., 2011). We thus interbred A20^{FL}ABIN-1^{FL} villin-ER/Cre⁺ mice with TNF^{-/-} mice and tested the responses of the resulting compound-mutant mice to tamoxifen. Remarkably, in contrast to the 100% mortality observed in tamoxifen-treated A20^{FL/FL}ABIN-1^{FL/+}TNF^{+/+} villin-ER/Cre⁺ mice, virtually all A20^{FL/FL}ABIN-1^{FL/+}TNF^{-/-} villin-ER/Cre⁺ mice survived (Fig. 2A). Consistent with this rescue, the intestinal epithelium from A20^{FL/FL}ABIN-1^{FL/+}TNF^{-/-} villin-ER/Cre⁺ mice was largely intact after tamoxifen treatment (Fig. 2, B and C). TNF deficiency also reduced the frequency of TUNEL-positive cells in A20^{FL/FL}ABIN-1^{FL/+}TNF^{-/-} villin-ER/Cre⁺ mice (Fig. 2, D and E). Hence, TNF triggers both IEC and organismal death in A20-deficient ABIN-1-heterozygous (A20^{FL/FL}ABIN-1^{FL/+}) villin-ER/Cre⁺ mice. In contrast, TNF deficiency failed to prevent the death of A20^{FL/FL}ABIN-1^{FL/FL} villin-ER/Cre⁺ mice (Fig. 2A). Therefore, extinction of ABIN-1 from A20-deficient IECs unveils acute TNF-independent mechanisms of organismal death *in vivo*.

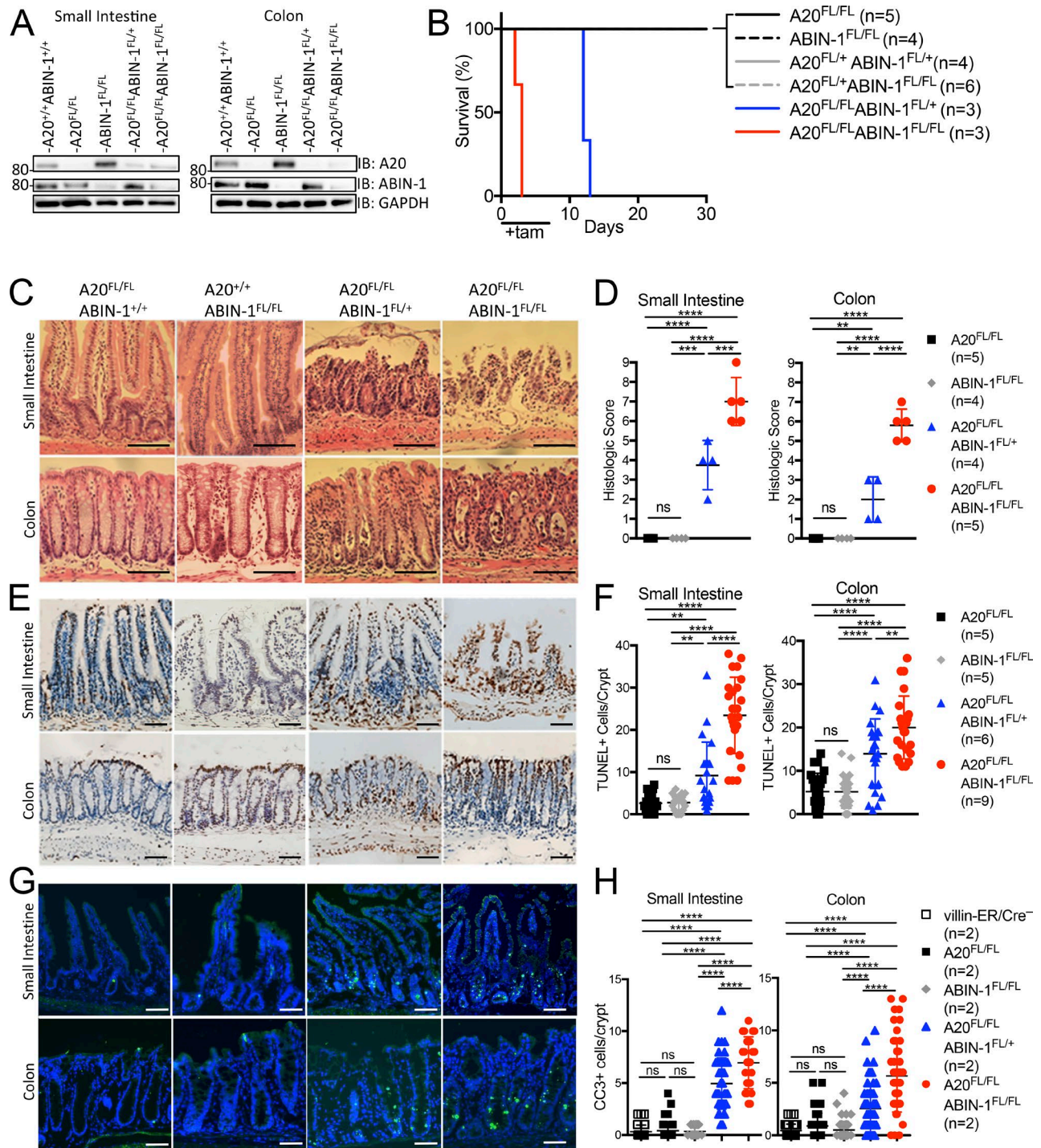


Figure 1. A20 and ABIN-1 cooperatively restrict intestinal epithelial apoptotic death in vivo. (A) Immunoblot of A20 and ABIN-1 in freshly isolated IEC lysates from the indicated genotypes of mice on the villin-ER/Cre⁺ background 40 h after initial tamoxifen injection. (B) Kaplan-Meier survival curves of the indicated genotypes of mice on the villin-ER/Cre⁺ background treated with tamoxifen (tam) for 5 d. (C) Representative H&E slides and (D) histological scoring of H&E-stained small intestinal and colonic sections 36 h after tamoxifen injection in mice with the indicated genotype; each data point represents one mouse (mean ± SD). The score ranges from 0 to 9, where no inflammation is 0 and the most severe inflammation is 9. (E) Representative TUNEL staining and (F) quantitation of TUNEL⁺ cells per villus of small intestinal and colonic sections 36 h after tamoxifen injection in mice with the indicated genotype; each data point represents one villus (mean ± SD). (G) Representative CC3 immunofluorescence and (H) quantitation of CC3⁺ cells per crypt from small intestinal and colonic sections 36 h after tamoxifen injection in mice with the indicated genotype; each data point represents one villus (mean ± SD). For D, F, and H statistical significance was assessed by one-way ANOVA with Tukey's multiple comparison test; *, P < 0.05; **, P < 0.01; ***, P < 0.001; ****, P < 0.0001. The number of mice in each group is indicated in the graph legends. Data are representative of at least two independent experiments. Bars, 50 μm.

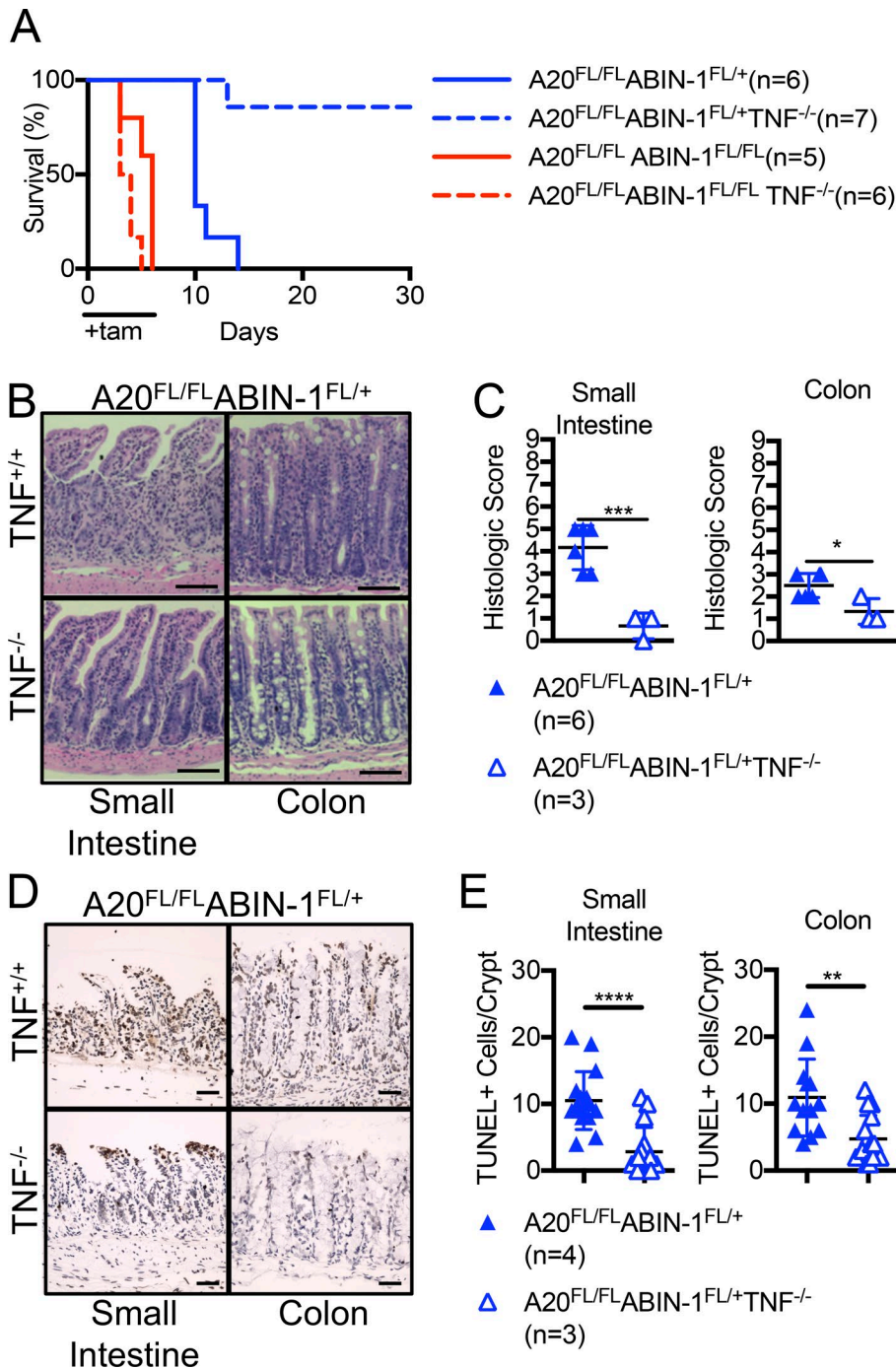


Figure 2. Mortality of A20^{FL/FL}ABIN-1^{FL/+} villin-ER/Cre⁺ mice involves both TNF-dependent and TNF-independent signals in vivo. (A) Kaplan-Meier survival curves after the indicated genotypes of mice on the villin-ER/Cre⁺ background were treated with tamoxifen for 5 d. The number of mice in each group is indicated in the graph legend. (B) Representative H&E sections and (C) cumulative histology scores from mice in A. Each data point represents one mouse (mean ± SD). (D) Representative TUNEL staining and (E) quantitation of TUNEL⁺ cells per villus of small intestinal and colonic sections 36 h after tamoxifen injection in A20^{FL/FL}ABIN-1^{FL/+} villin-ER/Cre⁺ mice; each data point represents one villus (mean ± SD). For C and E, the number of mice in each group is indicated in the graph legends, and statistical significance was assessed by two-tailed t test; *, P < 0.05; **, P < 0.01; ***, P < 0.001; ****, P < 0.0001. Data are representative of at least two independent experiments. Bars, 50 μm.

A20 and ABIN-1 cooperatively preserve IEC survival via an IEC-intrinsic mechanism

The data above suggest that acute deletion of A20 coupled with partial or complete deletion of ABIN-1 from IECs triggers a dramatic cascade of events that leads to rapid death of mice. IECs integrate responses from a number of host and microbial ligands in vivo. To determine the cell autonomous mechanisms by which A20 and ABIN-1 may preserve IEC survival in the absence of such ligands, we prepared intestinal enteroid IEC cultures from the small intestines of various genotypes of A20^{FL}ABIN-1^{FL} villin-ER/Cre⁺ mice. Treatment of these cultures with 4-hydroxytamoxifen (4-OHT) in vitro led to acute depletion of A20 and ABIN-1 proteins

within 24 h (Fig. 3 A). Notably, acute depletion of A20 caused marked up-regulation of ABIN-1 protein expression and vice versa (Fig. 3 A). This compensatory up-regulation is consistent with the idea that ABIN-1 may partially compensate for A20 deficiency. Furthermore, ABIN-1 protein levels in A20^{FL/FL}ABIN-1^{FL/+} villin-ER/Cre⁺ remained higher than in WT cells (Fig. 3 A).

We then assessed the sensitivity of these acutely deleted enteroid IECs to TNF-induced cell death. Death was assessed qualitatively via confocal microscopy of propidium iodide (PI)-stained enteroids and quantitatively by using an ATP-based luminescent cell viability assay (Fig. 3, B and C). To approximate physiological conditions, we avoided death-sensitizing agents (e.g.,

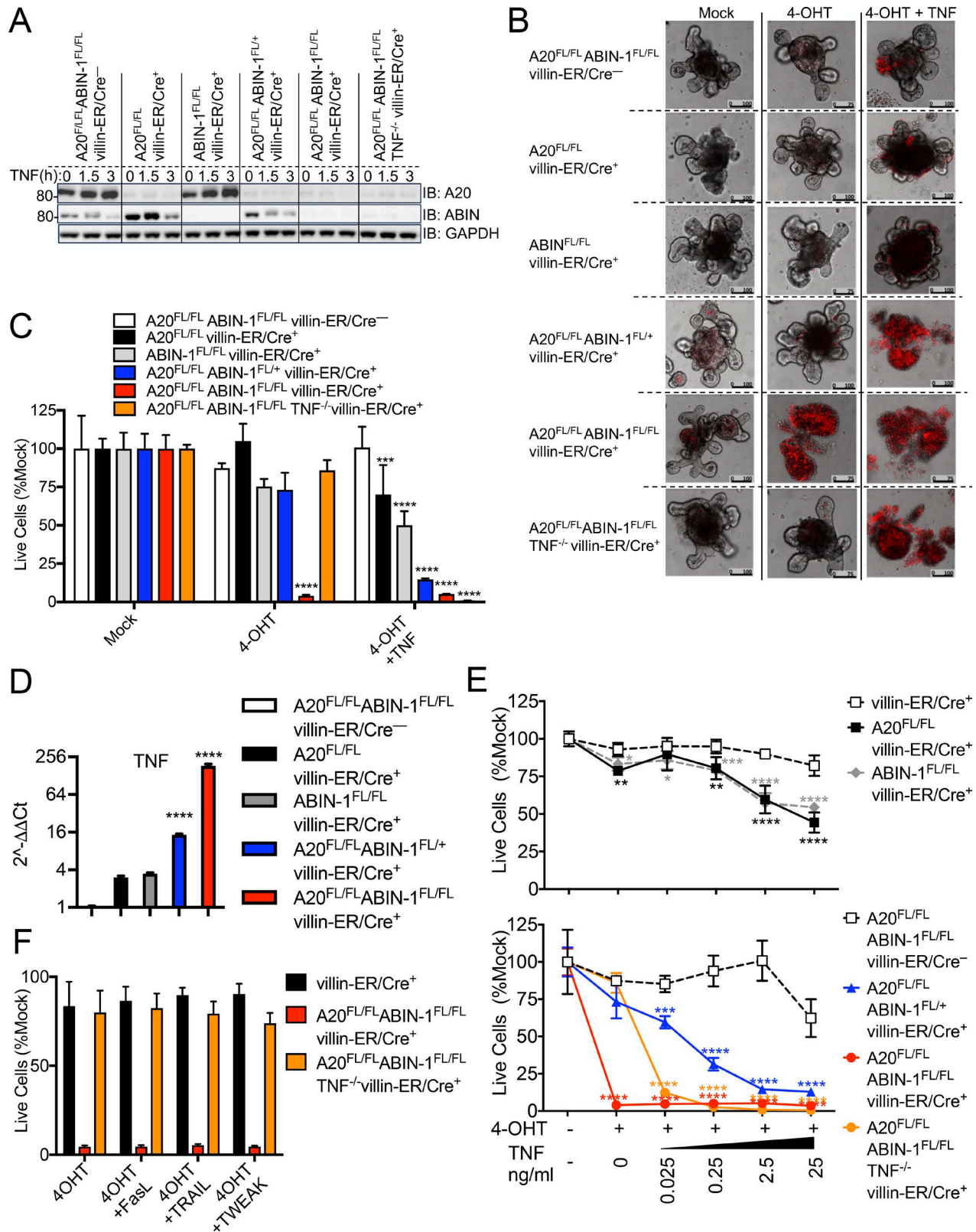


Figure 3. **Combined deletion of A20 and ABIN-1 sensitizes enteroids to TNF-induced cell death.** (A) Immunoblot analyses of A20 and ABIN-1 expression in enteroids isolated from villin-ER/Cre⁺ mice of the indicated genotypes and treated with 4-OHT for 24 h followed by stimulation with 2.5 ng/ml TNF for the indicated time points. (B) Representative confocal microscopy images of PI-stained enteroids from indicated genotypes of mice treated with 4-OHT for 24 h followed by 24 h of 2.5 ng/ml TNF versus mock treatment as indicated. Bars, 75 or 100 μm, as indicated. (C) Quantitation of cell viability of enteroid cultures described in B (mean ± SD). (D) qPCR analysis of TNF mRNA from enteroid cultures with the indicated genotypes after 24 h of 4-OHT treatment (mean ± SD). (E) Dose-response curve of TNF-induced cytotoxicity (mean ± SD). Cell viability of enteroids with the indicated genotypes treated for 24 h with 4-OHT followed

SMAC mimetics, cycloheximide). Addition of 4-OHT alone did not lead to significant spontaneous death of A20^{FL/FL} villin-ER/Cre⁺ (Fig. 3 C, black bars), ABIN-1^{FL/FL} villin-ER/Cre⁺ (Fig. 3 C, gray bars), or compound-mutant A20-deficient, ABIN-1-heterozygous enteroids (A20^{FL/FL}ABIN-1^{FL/+} villin-ER/Cre⁺; Fig. 3 C, blue bars) compared with control enteroids, although these IECs were sensitized to exogenous TNF (Fig. 3, B and C). Remarkably, treatment of A20^{FL/FL}ABIN-1^{FL/FL} villin-ER/Cre⁺ enteroid cultures (Fig. 3 C, red bars) with 4-OHT alone caused rapid spontaneous death (Fig. 3, B and C). Thus, homozygous loss of both A20 and ABIN-1 from IECs rapidly triggers the spontaneous death of these cells in the complete absence of luminal microbes or host immune cells. Death of A20 and ABIN-1 double-deficient IECs is therefore entirely IEC-intrinsic. Although prior studies have suggested that A20- and ABIN-1-deficient cells are sensitized to cell death in the setting of TNF and cycloheximide, this is the first study of spontaneous death upon deletion of both A20 and ABIN-1.

We next derived enteroids from TNF-deficient A20^{FL/FL}ABIN-1^{FL/FL} villin-ER/Cre⁺ mice and assessed their viability after inducing deletion with 4-OHT. Strikingly, A20^{FL/FL}ABIN-1^{FL/FL} TNF^{-/-} villin-ER/Cre⁺ enteroids (Fig. 3 C, orange bars) remained viable in contrast to their TNF^{+/+} counterparts (Fig. 3, B and C). Therefore, IEC-derived TNF is sufficient to induce death of A20^{FL/FL}ABIN-1^{FL/FL} villin-ER/Cre⁺ enteroids. It also indicates that A20^{FL/FL}ABIN-1^{FL/FL} villin-ER/Cre⁺ IECs spontaneously produce physiologically important amounts of TNF without any overt additional pathogenic or inflammatory stimulus, which was confirmed at the mRNA level (Fig. 3 D). The survival of A20^{FL/FL} ABIN-1^{FL/FL}TNF^{-/-} villin-ER/Cre⁺ IECs after 4-OHT treatment in vitro suggests that the TNF-independent death signals contributing to mortality of A20^{FL/FL} ABIN-1^{FL/FL} TNF^{-/-} villin-ER/Cre⁺ mice in vivo appear to be IEC-extrinsic.

To further compare the relative sensitivities of the various genotypes of IECs to TNF, we performed TNF-dose response studies (Fig. 3 E). A20^{FL/FL} villin-ER/Cre⁺ (Fig. 3 E, black curve) and ABIN-1^{FL/FL} villin-ER/Cre⁺ enteroids (Fig. 3 E, gray curve) were modestly sensitized to TNF compared with control enteroids (Fig. 3 E, top). Compound-mutant A20-deficient, ABIN-1-heterozygous enteroids (A20^{FL/FL}ABIN-1^{FL/+} villin-ER/Cre⁺; Fig. 3 E, blue curve) were >100 times more sensitive to TNF-induced cell death when compared with IECs lacking A20 or ABIN-1 alone (Fig. 3 E, bottom). Given that ABIN-1 protein expression is elevated above WT cells in A20^{FL/FL}ABIN-1^{FL/+} villin-ER/Cre⁺ cells (Fig. 3 A), it appears that elevated ABIN-1 expression partly compensates for A20 deficiency. Finally, these dose-response studies further revealed that TNF-deficient A20^{FL/FL}ABIN-1^{FL/FL} TNF^{-/-} villin-ER/Cre⁺ IECs (Fig. 3 E, orange lines) were >1,000

times more sensitive to TNF than singly deficient IECs and almost completely died in response to as little as 25 pg/ml of exogenous TNF (Fig. 3 E, bottom). This >1,000-fold increased sensitivity to TNF represents a potent synergistic relationship between A20 and ABIN-1.

Because TNF deficiency rescues A20 and ABIN-1 double-deficient IECs in vitro, but not in vivo, there appear to be IEC-extrinsic, TNF-independent, death signals that lead to lethality in vivo. To understand which factors might directly trigger TNF-independent death of IECs, we first stimulated A20^{FL/FL}ABIN-1^{FL/FL} TNF^{-/-} villin-ER/Cre⁺ enteroids with additional death-inducing ligands in vitro. The TNF superfamily members TWEAK (TNF-like weak inducer of apoptosis), Fas ligand, and TRAIL (TNF-related apoptosis inducing ligand) failed to induce significant death of A20^{FL/FL}ABIN-1^{FL/FL}TNF^{-/-} villin-ER/Cre⁺ IECs when compared with 4-OHT deletion alone (Fig. 3 F). To further investigate TNF-independent, IEC-extrinsic death in vivo, we hypothesized that microbial signals could directly or indirectly lead to IEC death in vivo. Broad-spectrum antibiotic treatment did not affect the survival of either A20^{FL/FL}ABIN-1^{FL/FL} villin-ER/Cre⁺ or A20^{FL/FL}ABIN-1^{FL/FL}TNF^{-/-} villin-ER/Cre⁺ mice (Fig. S1). To determine if IEC-extrinsic signals were hematopoietically derived, we irradiated A20^{FL/FL}ABIN-1^{FL/FL} villin-ER/Cre⁺ and A20^{FL/FL}ABIN-1^{FL/FL}TNF^{-/-} villin-ER/Cre⁺ mice and reconstituted these mice with MyD88^{-/-} or WT bone marrow cells. After hematopoietic reconstitution, these chimeric mice were treated with tamoxifen. Interestingly, MyD88^{-/-} but not WT hematopoietic cells rescued A20^{FL/FL}ABIN-1^{FL/FL}TNF^{-/-} villin-ER/Cre⁺ mice from tamoxifen-induced death (Fig. S2). This finding suggests that MyD88-dependent proteins from hematopoietic cells contribute to IEC death in A20^{FL/FL}ABIN-1^{FL/FL}TNF^{-/-} villin-ER/Cre⁺ mice. By contrast, MyD88^{-/-} hematopoietic cells did not rescue TNF-sufficient A20^{FL/FL}ABIN-1^{FL/FL} villin-ER/Cre⁺ mice. This result likely reflects expression of TNF by IECs, as seen in A20^{FL/FL}ABIN-1^{FL/FL} villin-ER/Cre⁺ enteroids. Overall, these data suggest that MyD88-dependent signals in hematopoietic cells contribute to IEC-extrinsic, TNF-independent death in A20^{FL/FL}ABIN-1^{FL/FL} TNF^{-/-} villin-ER/Cre⁺ mice.

A20 and ABIN-1 synergistically restrict caspase-dependent, RIPK3-independent, RIPK1 kinase-dependent apoptosis

Excessive apoptosis and/or necroptosis in IECs causes intestinal inflammation in mice lacking caspase 8 or RIPK1 (Günther et al., 2011, 2015; Dannappel et al., 2014; Takahashi et al., 2014). To better understand how A20 and ABIN-1 collaborate to restrict cell death in IECs, we studied cell death signaling in enteroid cultures. Single-mutant A20^{FL/FL} villin-ER/Cre⁺ IECs exhibited slightly increased CC3, CC8, cleaved poly (ADP-ribose)

by 24 h of TNF at the indicated concentrations versus mock treatment. Statistical significance was assessed by two-way ANOVA with Dunnett's multiple comparison test comparing the effect of each concentration to villin-ER/Cre⁻ or villin-ER/Cre⁺ enteroids as indicated. (F) Cell viability of organoids of the indicated genotypes treated with 4-OHT for 24 h followed by stimulation with TWEAK, FasL, or TRAIL for 24 h (mean ± SD). For C, E, and F, viability was measured by using the Cell-Titer Glo 3D assay, and data were normalized to mock-treated cells (%Mock). (C-E) Statistical significance was assessed by two-way ANOVA with Dunnett's multiple comparison test comparing the effect to villin-ER/Cre⁻ or villin-ER/Cre⁺ enteroids as indicated. (F) Statistical significance was assessed by two-way ANOVA with Dunnett's multiple comparison test comparing each stimulation to 4-OHT alone. *, P < 0.05; **, P < 0.01; ***, P < 0.001; ****, P < 0.0001. Data are representative of at least two independent experiments.

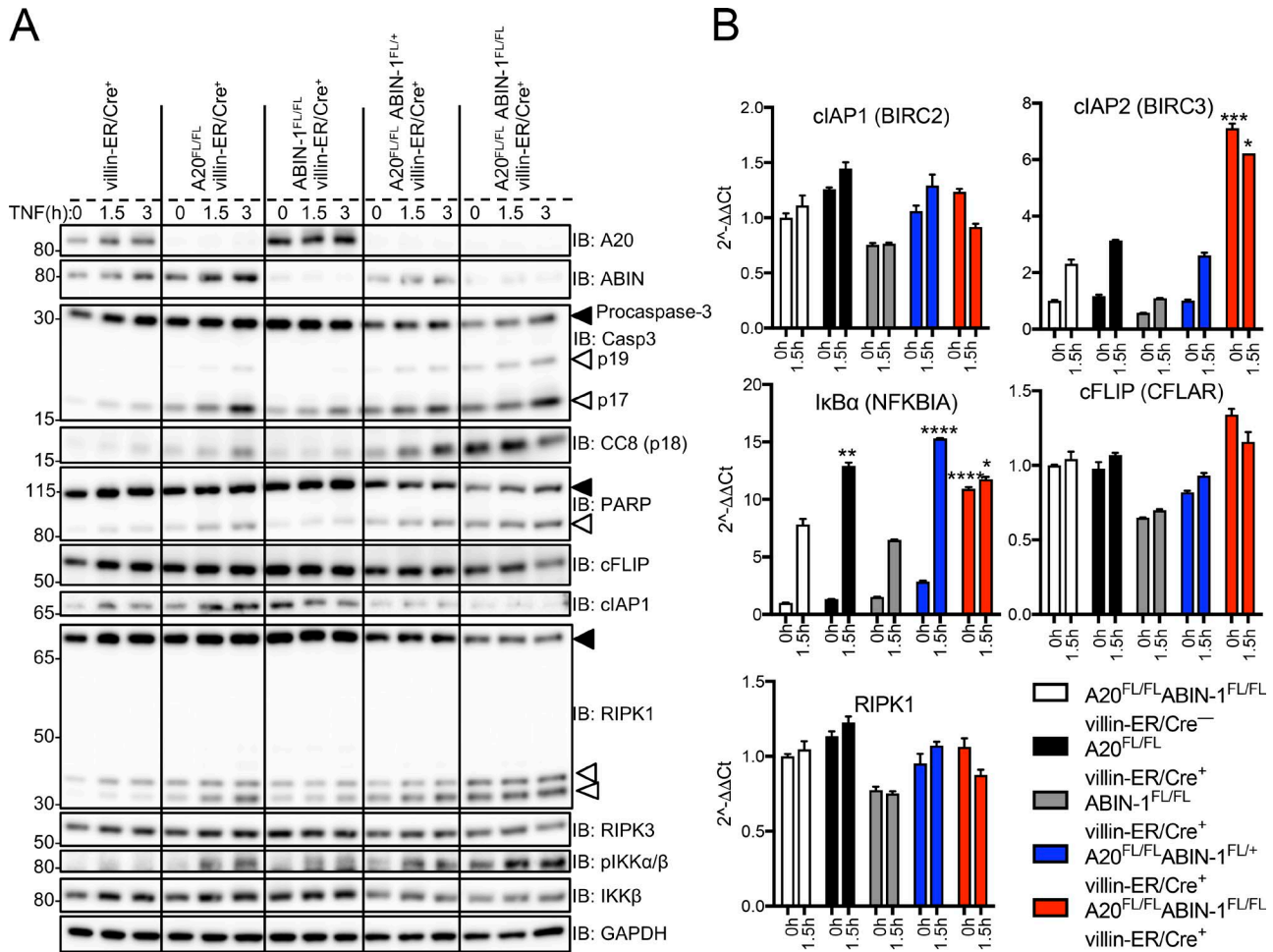


Figure 4. A20 and ABIN-1 double-deficient enteroids are sensitized to TNF-induced apoptosis. (A) Immunoblotting analyses of enteroid cultures treated with 4-OHT for 24 h followed by 2.5 ng/ml TNF for 0, 1.5, and 3 h. Cell lysates were immunoblotted with the antibodies indicated on the right. Solid arrow indicates full-length protein; open arrow indicates cleaved protein. **(B)** qPCR analyses of mRNA from enteroid cultures of the indicated genotypes after 24 h of 4-OHT treatment followed by stimulation for 0 or 90 min with 2.5 ng/ml TNF. Relative gene abundance was normalized to the mean expression of the housekeeping gene *actb* (mean \pm SD). Statistical significance for individual transcripts was assessed by two-way ANOVA with Dunnett's multiple comparison test comparing each genotype to villin-ER/Cre⁻ enteroids. *, $P < 0.05$; **, $P < 0.01$; ***, $P < 0.001$; ****, $P < 0.0001$. Data are representative of at least two independent experiments.

polymerase (PARP), and cleaved RIPK1, but normal cellular FLICE-inhibitory protein (cFLIP), cellular inhibitor of apoptosis protein (cIAP1), and RIPK3 compared with control IECs after 4-OHT mediated deletion and TNF stimulation (Fig. 4 A). Single-mutant ABIN-1^{FL/FL} villin-ER/Cre⁺ IECs exhibited normal amounts of caspase 3, caspase 8, PARP, cFLIP, cIAP1, RIPK1, and RIPK3 after 4-OHT mediated deletion and TNF stimulation (Fig. 4 A). By contrast, A20^{FL/FL}ABIN-1^{FL/+} villin-ER/Cre⁺ IECs and double-mutant A20^{FL/FL}ABIN-1^{FL/FL} villin-ER/Cre⁺ IECs contained markedly elevated amounts of CC3, CC8, cleaved PARP, and cleaved RIPK1, all of which are caspase 8 substrates (Fig. 4 A). These data suggest that A20 and ABIN-1 synergistically restrict caspase 8 activity and apoptotic signaling. In addition, double A20 and ABIN-1 mutant IECs contained lower amounts of the antiapoptotic proteins cFLIP and cIAP1, which could both result from, and contribute to, increased apoptosis sensitivity (Fig. 4 A; Wang et al., 2008; Feoktistova et al., 2011; Tenev et al., 2011). The deficiencies of cFLIP and cIAP1 protein expression are likely due to

posttranscriptional mechanisms, because mRNA levels of BIRC2 (cIAP1), BIRC3 (cIAP2), and CFLAR (cFLIP) were greater in A20^{FL/FL}ABIN-1^{FL/FL} villin-ER/Cre⁺ IECs than in normal or single-mutant cells (Fig. 4 B). More generally, NF- κ B activity, as reflected by mRNA levels of BIRC3 (cIAP2), NFKBIA (I κ B α), and TNF, was elevated in A20^{FL/FL}ABIN-1^{FL/FL} villin-ER/Cre⁺ IECs compared with control IECs (Figs. 3 D and 4 B). Phosphorylated I κ B-kinase α/β (IKK α/β) was also increased in the A20- and ABIN-1-deficient IECs, consistent with increased NF- κ B signaling (Fig. 4 A). Hence, deficient NF- κ B signaling and transcriptional induction of prosurvival proteins probably do not contribute to the death susceptibility of these cells. Taken together, these studies suggest that A20 and ABIN-1 cooperate to prevent IEC death by restricting caspase 8 activation and apoptotic signaling.

As A20 inhibits necroptosis as well as apoptosis (Lee et al., 2000; Onizawa et al., 2015), we investigated the degree to which these two pathways contribute to the death of A20^{FL/FL}ABIN-1^{FL/FL} villin-ER/Cre⁺ IECs. RIPK3 mediates caspase-independent

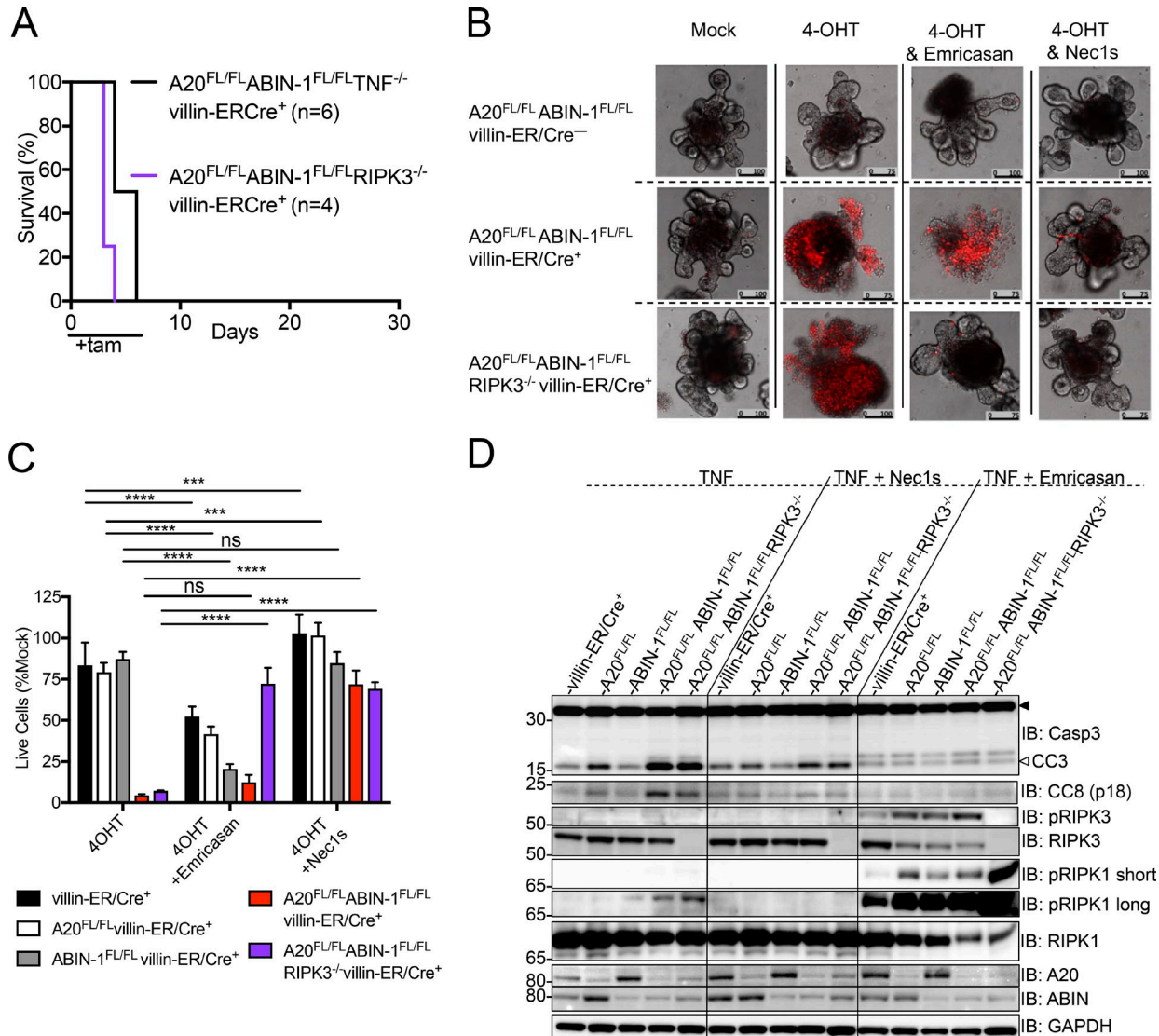


Figure 5. A20 and ABIN-1 double-deficient enteroids die primarily via caspase-dependent, RIPK1 kinase-dependent, RIPK3-independent apoptosis. (A) Kaplan-Meier survival curves of the indicated genotypes of mice treated with tamoxifen for 7 d. The number of mice is indicated in the graph legend. (B) Representative confocal microscopy images of PI-stained enteroids with the indicated genotypes treated for 48 h with 4-OHT with or without emricasan or Nec1s, versus mock, as indicated. Bars, 75 or 100 μ m, as indicated. (C) Quantitation of cell viability of enteroid cultures treated as indicated (mean \pm SD). Viability was measured by using the Cell-Titer Glo 3D assay, and data were normalized to unstimulated cells (%Mock). Statistical significance was assessed by two-way ANOVA with Dunnett's multiple comparison test comparing each stimulation to 4-OHT alone. *, $P < 0.05$; **, $P < 0.01$; ***, $P < 0.001$; ****, $P < 0.0001$. (D) Immunoblotting analyses of enteroid cultures treated with 4-OHT for 24 h in the presence of Nec1s or emricasan or Mock, followed by 0.25 ng/ml TNF for 3 h. Cell lysates were immunoblotted with the antibodies indicated on the right. Solid arrow indicates full-length protein; the open arrow indicates cleaved protein. Data are representative of at least two independent experiments.

necroptosis. RIPK3 deficiency did not rescue A20 and ABIN-1 double-deficient mice (Fig. 5 A and data not depicted). Additionally, enteroids derived from A20^{FL/FL}ABIN-1^{FL/FL}RIPK3^{-/-} villin-ER/Cre⁺ mice (Fig. 5 C, purple bars) died similarly to A20^{FL/FL}ABIN-1^{FL/FL} villin-ER/Cre⁺ IECs (Fig. 5 C, red bars), confirming that these IECs die predominantly via RIPK3-independent apoptotic cell death (Fig. 5, B and C). In agreement with this, TNF stimulation of A20^{FL/FL}ABIN-1^{FL/FL} villin-ER/Cre⁺ and A20^{FL/FL}ABIN-1^{FL/FL}RIPK3^{-/-} villin-ER/Cre⁺ enteroids induced increased caspase 3 and caspase 8 cleavage compared with A20 or ABIN deletion alone, indicating increased RIPK3-independent apoptotic death signaling (Fig. 5 D). Phospho-RIPK3, a marker of

necroptotic cell death, was not seen by immunoblot in any of the enteroids stimulated with TNF alone (Fig. 5 D). RIPK3-dependent necroptosis is therefore dispensable for death of A20 and ABIN-1 double-deficient IECs both in vitro and in vivo.

To further dissect the death-signaling mechanisms in A20- and ABIN-1-deficient cells, we used emricasan, a pharmacologic pan-caspase inhibitor, and assessed both cell viability and downstream signaling (Fig. 5, B-D). Treatment of enteroid cultures with 4-OHT and emricasan did not rescue A20^{FL/FL}ABIN-1^{FL/FL} villin-ER/Cre⁺ IECs (Fig. 5, B and C, red bars) and actually induced more spontaneous cell death of control (Fig. 5, B and C, black bars), A20-deficient (Fig. 5, B and C, white bars), and ABIN-1-deficient enteroids

(Fig. 5, B and C, gray bars). A20^{FL/FL}ABIN-1^{FL/FL}RIPK3^{-/-} villin-ER/Cre⁺ enteroids, in stark contrast, were significantly rescued by emricasan (Fig. 5, B and C, purple bars). Genetic and pharmacologic inhibition of caspases drives cells toward caspase-independent, RIPK3-dependent necroptotic cell death characterized by increased phosphorylation of RIPK3. The increased susceptibility to TNF and emricasan induced cell death of A20 and ABIN-1 double-deficient enteroids correlated biochemically with increased phospho-RIPK3 by immunoblot (Fig. 5 D). Of note, emricasan completely abrogated CC3 and CC8 in all enteroids (Fig. 5 D). A20 and ABIN-1 double-deficient cells therefore die primarily via caspase-dependent apoptosis, but they are not rescued by caspase inhibition because of an increased susceptibility to necroptosis. As a result, combined blockade of apoptosis and necroptosis is required to rescue A20 and ABIN-1 double-deficient IECs from TNF-induced cell death.

RIPK1 binds caspase 8, and RIPK1's kinase activity can support both apoptotic and necroptotic death (Dondelinger et al., 2013; Dannappel et al., 2014; Vlantis et al., 2016; Kondylis et al., 2017). To study the contribution of RIPK1 kinase activity in our enteroid cultures, we used Necrostatin-1s (Nec1s). Nec1s is a small-molecule RIPK1 kinase inhibitor that is 1,000-fold more selective for RIPK1 compared with 485 human kinases and lacks any activity on indoleamine 2,3-dioxygenase (Takahashi et al., 2012). Treatment of enteroid IECs with 4-OHT and the RIPK1 kinase inhibitor revealed that A20^{FL/FL}ABIN-1^{FL/FL} villin-ER/Cre⁺ IECs were markedly protected by RIPK1 kinase inhibition (Fig. 5, B and C, red bars). Combined A20/ABIN-1 deficiency therefore renders IECs susceptible to RIPK1 kinase activity-dependent death. Nec1s prevented spontaneous death equally effectively in A20^{FL/FL}ABIN-1^{FL/FL} villin-ER/Cre⁺ (Fig. 5, B and C, red bars) and A20^{FL/FL}ABIN-1^{FL/FL}RIPK3^{-/-} villin-ER/Cre⁺ IECs (Fig. 5, B and C, purple bars), demonstrating that Nec1s inhibits apoptosis in these cells, rather than rescuing necroptosis. Signaling studies in Nec1s-treated IECs reinforced this notion because Nec1s reduced CC3 and CC8 in A20^{FL/FL}ABIN-1^{FL/FL} villin-ER/Cre⁺ IECs (Fig. 5 D). We observed significantly more phospho-RIPK1 in A20 and ABIN-1 double-deficient enteroids compared with enteroids deficient in either A20 or ABIN-1 after stimulation with TNF alone (Fig. 5 D). RIPK1 undergoes autophosphorylation (Newton et al., 2016), and phospho-RIPK1 was completely inhibited along with caspase cleavage in cells stimulated with TNF and Nec1s (Fig. 5 D). Taken together, these studies indicate that A20 and ABIN-1 cooperatively restrict RIPK1 kinase activity, which in turn restricts apoptotic cell death. Therefore, A20^{FL/FL}ABIN-1^{FL/FL} villin-ER/Cre⁺ IECs die primarily via TNF-, caspase 8-, and RIPK1 kinase-dependent apoptosis, with minimal contribution from RIPK3-dependent necroptosis, except under conditions in which apoptosis is inhibited.

Discussion

Overall, our studies highlight a broad new mechanism by which A20 and ABIN-1 cooperatively prevent inflammatory disease. Whereas previous studies have revealed important mechanisms by which these proteins prevent inflammation by restricting immune cell activation, our current results reveal that A20 and ABIN-1 play profound roles in preserving IEC survival in a

cell-autonomous fashion. The ability of these proteins to both restrict immune cell activation and protect epithelial cell survival may help explain why they are such potent and pleiotropic disease susceptibility proteins. Exaggerated inflammation could initiate tissue damage and increase the sensitivity of stromal cells to inflammatory mediators, which in turn could cause exaggerated cell death and mucosal ulceration. This tissue damage would then elicit recruitment of more immune cells in a pathogenic feed-forward cycle (Cummings et al., 2016). A20 and ABIN-1 expression could thus become compelling biomarkers as well as therapeutic targets. Additionally, this study highlights the fact that examining genetic interactions is critical to understand how multigenic disorders such as IBD arise from the presence of multiple risk alleles, each conferring modest relative risk individually.

We have discovered a surprising epistatic relationship between A20 and ABIN-1. ABIN-1 appears to function in a dose-dependent manner to compensate for A20 deficiency in supporting cell survival. This observation raises several novel implications. First, in contrast to a signaling model in which ABIN-1 functions as an adaptor for A20 and A20's enzymatic functions, ABIN-1 must perform critical A20-independent survival functions. These functions may be nonenzymatic, because ABIN-1 is not known to exhibit ubiquitin-modifying enzymatic activity. However, they may readily involve regulating the behavior of ubiquitinated signaling complexes, because ABIN-1 binds to ubiquitin. Second, the compensatory increase of ABIN-1 expression in A20-deficient cells suggests that previous studies of A20 deficiency underestimate the cellular and physiological impact of losing shared A20/ABIN-1-dependent signaling functions. The synergy between A20 and ABIN-1 could also impact signaling functions other than cell death signaling. Hence, further studies using compound-mutant cells could reveal the fuller extent of the biological impact of these proteins. This notion carries significant clinical impact given the links between these two proteins and human disease.

In the context of IEC survival, we have found that A20 and ABIN-1 cooperatively restrict caspase-dependent, RIPK1 kinase-dependent, and RIPK3-independent TNF-induced cell death. We observed increased caspase 8 activity and increased RIPK1 kinase activity in A20- and ABIN-1-deficient cells. A20 modulates the ubiquitination states of multiple proximate cell death-signaling molecules including caspase 8, RIPK1, and RIPK3, which in turn modulates their activity (Jin et al., 2009; Onizawa et al., 2015). ABIN-1 regulates the association of these same proteins and prevents RIPK1-dependent death (Oshima et al., 2009; Dziedzic et al., 2018). ABIN-1 inhibits caspase 8 recruitment to Fas-associated death domain-containing protein (FADD) (Oshima et al., 2009), and it is possible that the combination of A20 and ABIN-1 deficiency further increases caspase-8/FADD interaction. We observed that A20 and ABIN-1 double-deficient IECs had lower cIAP1 after TNF stimulation, and A20 has been reported to bind cIAP1 (Yamaguchi and Yamaguchi, 2015), so it is also possible that the combined A20 and ABIN-1 deficiency directly causes IAP loss and thereby increases susceptibility to cell death. A20 and ABIN-1 may also regulate distinct ubiquitination events of RIPK1, and these RIPK1 ubiquitination events influence RIPK1 phosphorylation and RIPK1 kinase activity (Wertz et al., 2004; Justus and Ting, 2015; de Almagro et al., 2017;

Dziedzic et al., 2018). Given our findings that A20 and ABIN-1 cooperatively restrict RIPK1 kinase activity, RIPK1 phosphorylation, and RIPK1 kinase-dependent apoptosis, A20 and ABIN-1 may synergistically regulate ubiquitination of RIPK1-bearing death-signaling complexes. These events would impact downstream death signaling and cell survival. Defects in autophagy can also increase susceptibility to cell death, including IEC death (Matsuzawa-Ishimoto et al., 2017), and A20 regulates autophagy in CD4⁺ T cells (Matsuzawa et al., 2015), so dysregulated autophagy in A20 and ABIN-1 double-deficient IECs could increase sensitivity to death. Dissecting these cell biological mechanisms will likely require coimmunoprecipitation, mass spectrometry, and other studies in more robust IEC cell lines. Further studies of A20, ABIN-1, and TNF signaling in human as well as mouse IECs should yield important clinical as well as biological insights.

A20 inhibits TNF-induced apoptosis in fibroblasts, blocks necroptosis in fibroblasts and T cells, and paradoxically promotes Fas-dependent death in activated B cells (Lee et al., 2000; Tavares et al., 2010; Onizawa et al., 2015). Hence, integration of cellular activation and cell survival signals occurs differently in distinct cell types. Our current studies reveal that primary, nontransformed, IECs exhibit unusual sensitivity to TNF and highlight enteroids as a powerful tool for more closely approximating *in vivo* biology. Unlike fibroblasts or model cell lines that we have tested, A20- and/or ABIN-1-deficient enteroid IECs do not require death sensitizers such as cycloheximide or SMAC mimetics to die in response to low (picogram) amounts of TNF. Hence, the mechanisms of IEC death that we have dissected harbor fewer caveats associated with *in vitro* studies and should be highly physiological. Additionally, we clearly demonstrate that intestinal enteroid cultures, devoid of hematopoietic cells and microbes, produce small but physiologically critical amounts of autocrine TNF sufficient to kill IECs. Further defining which IEC subsets are most susceptible to TNF-induced cell death in the setting of A20 and/or ABIN-1 deficiency could yield additional important translational insights. Anti-TNF therapy has been reported to decrease apoptotic IEC frequency in IBD patients (Zeissig et al., 2004), raising the possibility that anti-TNF therapy may inhibit autocrine TNF produced by IECs, thereby inhibiting mucosal injury and inflammation.

RIPK1 kinase inhibitors are currently in clinical trials for UC (Weisel et al., 2017). RIPK1 kinase inhibition does not broadly inhibit NF κ B, so these inhibitors would likely be less immunosuppressive than other agents currently used to treat patients with IBD (Dannappel et al., 2014; Berger et al., 2015). Here we show that inhibiting RIPK1 kinase activity in the setting of A20 and ABIN-1 deficiency can inhibit both apoptosis and necroptosis. The biochemical signature of lower A20 and ABIN-1 in mucosal biopsies might therefore identify a subset of patients that could respond particularly well to RIPK1 kinase inhibition. In general, current immunosuppressive therapies target hematopoietic cells. Co-administering immunosuppressive agents with agents that protect the target tissue from injury, such as RIPK1 inhibitors, may emerge as a paradigm for how we can effectively treat patients with refractory autoimmune or auto-inflammatory disease without exposing them to unnecessary infectious complications.

In summary, we have discovered an unexpected epistatic relationship between the disease-modifying proteins A20 and ABIN-1. Instead of serving strictly as an adaptor for A20, ABIN-1 protects IEC survival in A20-deficient cells. Hence, ABIN-1 protects IEC survival in an A20-independent fashion. Moreover, ABIN-1 appears to compensate for A20 deficiency in a dose-dependent fashion. The potent shared function of these proteins in regulating ubiquitin-dependent cell survival signals unveils a critical facet of IEC homeostasis. Ultimately, preservation of intestinal epithelial integrity is critical to mucosal healing and restoring homeostasis. The pleiotropic expression of both proteins and their links to multiple autoimmune and inflammatory diseases suggest that A20 and ABIN-1 may broadly prevent tissue damage in addition to suppressing immune activation.

Materials and methods

Mice

A20^{FL} and ABIN^{FL} mice were generated in our laboratory and were described previously (Tavares et al., 2010; Callahan et al., 2013; Lu et al., 2013; Onizawa et al., 2015). TNF^{-/-} and MyD88^{-/-} mice were purchased from Jackson Laboratories and backcrossed to A20 and ABIN transgenic mice for more than eight generations. X. Wang (National Institute of Biological Sciences, Beijing, China) provided RIPK3^{-/-} mice. Transgenic mice harboring a tamoxifen-inducible Cre recombinase under the control of the villin-promoter (villin-ER/Cre) were a gift from S. Robine (Institut Curie-CNRS, Paris, France; el Marjou et al., 2004). Acute deletion of floxed A20 and ABIN-1 exons *in vivo* was performed by daily intraperitoneal injection of 1 mg tamoxifen (1 mg/d, T5648; Sigma Aldrich) for 5–7 consecutive days as indicated. To generate radiation bone marrow chimeras, mice were irradiated with 1,200 rads total body radiation, reconstituted with 5 × 10⁶ bone marrow cells injected via the retroorbital vein within 1 h of irradiation and allowed to recover for 6 wk before tamoxifen injection. For antibiotic treatment, mice were treated with ampicillin 1 mg/ml (Sigma Aldrich), vancomycin 0.5 mg/ml (Sigma Aldrich), metronidazole 1 mg/ml (Sigma Aldrich), and neomycin 1 mg/ml (Sigma Aldrich) in double-distilled H₂O starting 7 d before tamoxifen injection and continued throughout the duration of tamoxifen injection. All animal studies were conducted in accordance with the University of California, San Francisco Institutional Animal Care and Use Committee. When possible, littermates were used as controls. Mice were analyzed between 4 and 8 wk of age for all experiments, with the exception of radiation chimera mice, which were 10–12 wk of age at the time of tamoxifen injection.

IEC enteroid culture and confocal microscopy

To confirm deletion of A20 and ABIN-1 in various villin-ER/Cre⁺ mice, IECs were isolated from the small intestine and colon at 40 h after the first injection of tamoxifen and purified as previously described (Shao et al., 2013). For enteroid culture, intestinal crypts were isolated from the small intestine as previously described (Sato and Clevers, 2012), with the modifications of substituting 10% R-spondin-1 conditioned medium for recombinant R-spondin1 and the addition of Normocin (100 mg/ml;

InviGen). R-spondin1 expressing 293T cells were a gift from N. Shroyer (Baylor College of Medicine, Houston, TX). For all enteroid experiments, enteroids were derived from at least three separate mice on separate occasions and representative data are shown. Deletion of A20 or ABIN-1 was performed via treatment with 4-OHT (250 nM; Sigma Aldrich). Confocal imaging of enteroids was performed on a Leica SP5 laser-scanning confocal system (Leica Microsystems) by using a 10× dry objective. Images were acquired in a format of 512 × 512, with a line mean of at least 3, scan speed of 400 Hz, and pinhole airy unit 1. Excitation for both PI and brightfield was done with the 488-nm laser line at 30% power with a detection band of 550–732 nm. Image analysis was performed on the Leica Application Suite (Leica Microsystems).

Antibodies and reagents

Antibodies directed against A20 (5630; Cell Signaling), ABIN-1 (HPA037893; Sigma Aldrich), c-IAP1 (ALX-803-335; Enzo and 4952; Cell Signaling), caspase 8 (9496, 4790; Cell Signaling and 804-429, Enzo), CC8 (8592, Cell Signaling), RIPK1 (3493; Cell Signaling), caspase 3 (9662; Cell Signaling), CC3 (9661; Cell Signaling), PARP (9532 and 9542; Cell Signaling), cFLIP (56343; Cell Signaling), mouse RIPK3 (95702; Cell Signaling), phospho-RIPK3 (T231/S232; ab205421; Abcam), phospho-RIPK1 (Ser166) rodent specific (31122; Cell Signaling), IKKβ (8943; Cell Signaling), phospho-IKKα/β (2697; Cell Signaling), and GAPDH (MAB374; Millipore) were used for Western blot as described below. Recombinant mouse TNF-α was purchased from R&D. Recombinant TWEAK (R&D) and TRAIL (Peprotech), were used at a final concentration of 250 ng/ml. FasL (R&D) was used at a final concentration of 40 ng/ml with anti-HA at 2.5 μg/ml (BioLegend). Nec1s (2263; BioVision) and emricasan (HY-10396; MedChemExpress) were used at 50 μM final concentration.

Cell death assays

Enteroid death assays were performed by resuspending in Matrigel (Corning) and plating 25 μl per well in 96-well flat-bottom opaque plates (Nunc). After 24 h, enteroids were stimulated as indicated to a final volume of 200 μl. Viability was measured by using the CellTiter Glo 3D assay (Promega) according to the manufacturer specifications, with the exception that 100 μl of reagent was added to 200-μl culture for a final volume of 300 μl before reading. Luminescence was read on a SpectraMax M5 (Molecular Devices) and analyzed by using SoftMax Pro (Molecular Devices).

Cell signaling assays and immunoblot analysis

For enteroid lysates, cultures were resuspended in Cell Recovery Solution (Corning) supplemented with 10 μM Y-27632 (Calbiochem) and incubated for 15 min on ice, followed by centrifugation at 550 g for 5 min. Cell pellets were lysed in ice-cold NP-40 lysis buffer (1% vol/vol NP-40, 50 mM Tris HCl pH 7.4, 150 mM NaCl, and 10% vol/vol glycerol) supplemented with complete EDTA-Free Protease Inhibitor Cocktail (Roche), phosphatase inhibitors (1 mM Na₃VO₄ and 10 mM NaF), and 10 mM *N*-ethylmaleimide. After lysis, samples were centrifuged for 20 min at 21,130 g to remove debris, and the supernatants were quantitated by using the BCA Protein Assay Kit (Pierce). Lysates were normalized and

denatured in LDS Sample Buffer (Invitrogen), followed by resolution on NuPage precast 4–12% Bis-Tris gels (Invitrogen) and transferred to polyvinylidene difluoride for immunoblotting.

Quantitative PCR (qPCR)

Enteroid cultures were resuspended in Cell Recovery Solution (Corning) supplemented with 10 μM Y-27632 (Calbiochem) and incubated for 15 min on ice. Total RNA was isolated with the PicoPure RNA Isolation Kit (Thermo Fisher Scientific) according to manufacturer instructions with on-column DNase I digestion (Qiagen). 500 ng total RNA was used for cDNA synthesis by using the High Capacity RNA-to-cDNA kit (Thermo Fisher Scientific). qPCR was performed by using TaqMan probes for mouse NFKBIA (Mm00477798_m1), mouse TNF (Mm99999068_m1), mouse RIPK1 (Mm00436354_m1), mouse CFLAR (Mm01255578_m1), mouse BIRC2 (Mm00431811_m1), mouse BIRC3 (Mm00431800_m1), mouse ACTB (Mm02619580_g1), and the TaqMan Universal Master Mix II with UNG on the QuantStudio 6 (Thermo Fisher Scientific). Relative gene abundance was normalized to the mean expression of the housekeeping gene *actb* and then compared with villin-ER/Cre⁻ at time 0 h as a reference for mouse enteroid experiments, and 2^{-ΔΔCt} was calculated. All samples were run in duplicate. Data were analyzed by using QuantStudio RealTime PCR Software (Thermo Fisher Scientific).

Immunohistochemistry and immunofluorescence

Resected intestinal tissue was fixed in 10% neutral-buffered formalin (Sigma Aldrich). Tissue specimens were then embedded in paraffin and stained according to standard protocols. Immunohistochemistry was performed at the University of California, San Francisco Cancer Center Core facility. Imaging for H&E- and TUNEL-stained slides were all obtained by using the 20× objective. H&E quantitation was performed by using a scoring system previously described (Burns et al., 2001). For CC3 immunofluorescence, mice were euthanized, the right atrium was lacerated, and 10 ml of PBS followed by 5 ml of 4% formaldehyde in PBS was injected into the left ventricle. The dissected intestine was placed in 4% formaldehyde in PBS and then embedded in Tissue-Tek OCT compound (Sakura) for sectioning. Antigen retrieval was performed in pH 6.0 citrate buffer microwaved for 10 min before applying first antibody. Slides were first probed with CC3 antibody (9664; Cell Signaling) and then biotinylated goat anti rabbit antibody (BA-1000; Vector), and then signal amplification was performed by using the ABC kit (Vector) and TSA fluorescence system (PerkinElmer) according to manufacturer instructions. Slides were visualized by using the 10× objective on the Olympus Ix-70 wide-field microscope.

Statistical analysis

Statistical analysis was performed with GraphPad Prism 4 (GraphPad Software). Comparisons between two groups were performed by two-tailed unpaired Student's *t* test. Multigroup comparisons were performed by ANOVA if we were comparing one variable per group or two-way ANOVA if there were multiple variables per group. When comparing each mean to every other mean by ANOVA, Tukey's multiple comparison test was used. When comparing each mean to a control, Dunnett's multiple

comparison test was used. $P < 0.05$ was used as the threshold for statistical significance. All experiments shown are representative of at least two independent repetitions.

Online supplemental material

Fig. S1 shows the survival curves of mice treated with antibiotics beginning 7 d before tamoxifen injection. Fig. S2 shows the survival curves of mice irradiated and reconstituted with either WT or MyD88-deficient bone marrow, followed by tamoxifen injection.

Acknowledgments

We thank Ophir Klein and Thad Stappenbeck for assistance with enteroid cultures.

This work was supported by the National Institutes of Health (NIH) grant DK095693, the Kenneth Rainin Foundation, and the Crohn's and Colitis Foundation. M.G. Kattah was initially supported by NIH grant T32 DK007007 and subsequently by a Career Development Award from the Crohn's and Colitis Foundation. L. Shao was initially supported by NIH grant T32 DK007007 and subsequently by KO8 DK100462.

The authors declare no competing financial interests.

Author contributions: M.G. Kattah, L. Shao, B.A. Malynn, and A. Ma made the *in vitro* and *in vivo* observations that led to this study. M.G. Kattah and L. Shao designed and performed the *in vivo* and *in vitro* experiments. Y.Y. Rosli assisted with all of the enteroid studies and some of the *in vivo* studies. H. Shimizu performed the CC3 immunofluorescence analysis. M.I. Wang assisted with mouse experiments. B.H. Duong and M. Onizawa assisted with some signaling studies. R. Advincula managed mouse breeding. P. Tanbun, S. Shah, and P. Achacoso assisted with mouse breeding and molecular analyses. B.A. Malynn and A. Ma oversaw studies. M.G. Kattah, B.A. Malynn, and A. Ma wrote the manuscript.

Submitted: 30 January 2018

Revised: 12 April 2018

Accepted: 7 June 2018

References

Arsenescu, R., M.E.C. Bruno, E.W. Rogier, A.T. Stefk, A.E. McMahan, T.B. Wright, M.S. Nasser, W.J.S. de Villiers, and C.S. Kaetzel. 2008. Signature biomarkers in Crohn's disease: Toward a molecular classification. *Mucosal Immunol.* 1:399–411. <https://doi.org/10.1038/mi.2008.32>

Berger, S.B., P. Harris, R. Nagilla, V. Kasparcova, S. Hoffman, B. Swift, L. Dare, M. Schaeffer, C. Capriotti, M. Ouellette, et al. 2015. Characterization of GSK'963: A structurally distinct, potent and selective inhibitor of RIP1 kinase. *Cell Death Discov.* 1:15009. <https://doi.org/10.1038/cddiscovery.2015.9>

Boone, D.L., E.E. Turer, E.G. Lee, R.-C. Ahmad, M.T. Wheeler, C. Tsui, P. Hurley, M. Chien, S. Chai, O. Hitotsumatsu, et al. 2004. The ubiquitin-modifying enzyme A20 is required for termination of Toll-like receptor responses. *Nat. Immunol.* 5:1052–1060. <https://doi.org/10.1038/ni110>

Bosanac, I., I.E. Wertz, B. Pan, C. Yu, S. Kusam, C. Lam, L. Phu, Q. Phung, B. Maurer, D. Arnott, et al. 2010. Ubiquitin binding to A20 ZnF4 is required for modulation of NF- κ B signaling. *Mol. Cell.* 40:548–557. <https://doi.org/10.1016/j.molcel.2010.10.009>

Bruno, M.E.C., E.W. Rogier, R.I. Arsenescu, D.R. Flomenhoft, C.J. Kurkjian, G.I. Ellis, and C.S. Kaetzel. 2015. Correlation of biomarker expression in colonic mucosa with disease phenotype in Crohn's disease and ulcerative colitis. *Dig. Dis. Sci.* 60:2976–2984. <https://doi.org/10.1007/s10620-015-3700-2>

Burns, R.C., J. Rivera-Nieves, C.A. Moskaluk, S. Matsumoto, F. Cominelli, and K. Ley. 2001. Antibody blockade of ICAM-1 and VCAM-1 ameliorates inflammation in the SAMP-1/Yit adoptive transfer model of Crohn's disease in mice. *Gastroenterology.* 121:1428–1436. <https://doi.org/10.1053/gast.2001.29568>

Callahan, J.A., G.E. Hammer, A. Agelides, B.H. Duong, S. Oshima, J. North, R. Advincula, N. Shifrin, H.-A. Truong, J. Paw, et al. 2013. Cutting edge: ABIN-1 protects against psoriasis by restricting MyD88 signals in dendritic cells. *J. Immunol.* 191:535–539. <https://doi.org/10.4049/jimmunol.1203335>

Catrysse, L., L. Vereecke, R. Beyaert, and G. van Loo. 2014. A20 in inflammation and autoimmunity. *Trends Immunol.* 35:22–31. <https://doi.org/10.1016/j.it.2013.10.005>

Cummings, R.J., G. Barbet, G. Bongers, B.M. Hartmann, K. Gettler, L. Muniz, G.C. Furtado, J. Cho, S.A. Lira, and J.M. Blaser. 2016. Different tissue phagocytes sample apoptotic cells to direct distinct homeostasis programs. *Nature.* 539:565–569. <https://doi.org/10.1038/nature20138>

Dannappel, M., K. Vlantis, S. Kumari, A. Polykratis, C. Kim, L. Wachsmuth, C. Eftychi, J. Lin, T. Corona, N. Hermance, et al. 2014. RIPK1 maintains epithelial homeostasis by inhibiting apoptosis and necroptosis. *Nature.* 513:90–94. <https://doi.org/10.1038/nature13608>

Das, T., Z. Chen, R.W. Hendriks, and M. Kool. 2018. A20/Tumor necrosis factor α -induced protein 3 in immune cells controls development of autoinflammation and autoimmunity: Lessons from mouse models. *Front. Immunol.* 9:104. <https://doi.org/10.3389/fimmu.2018.00104>

de Almagro, M.C., T. Goncharov, A. Izrael-Tomasevic, S. Duttler, M. Kist, E. Varfolomeev, X. Wu, W.P. Lee, J. Murray, J.D. Webster, et al. 2017. Coordinated ubiquitination and phosphorylation of RIP1 regulates necroptotic cell death. *Cell Death Differ.* 24:26–37. <https://doi.org/10.1038/cdd.2016.78>

Di Narzo, A.F., L.A. Peters, C. Argmann, A. Stojmirovic, J. Perrigou, K. Li, S. Telesco, B. Kidd, J. Walker, J. Dudley, et al. 2016. Blood and intestine eQTLs from an anti-TNF-resistant Crohn's disease cohort inform IBD genetic association loci. *Clin. Transl. Gastroenterol.* 7:e177. <https://doi.org/10.1038/ctg.2016.34>

Dondelinger, Y., M.A. Aguilera, V. Goossens, C. Dubuisson, S. Grootjans, E. Dejardin, P. Vandenabeele, and M.J.M. Bertrand. 2013. RIPK3 contributes to TNFR1-mediated RIPK1 kinase-dependent apoptosis in conditions of cIAP1/2 depletion or TAK1 kinase inhibition. *Cell Death Differ.* 20:1381–1392. <https://doi.org/10.1038/cdd.2013.94>

Dziedzic, S.A., Z. Su, V. Jean Barrett, A. Najafov, A.K. Mookhtiar, P. Amin, H. Pan, L. Sun, H. Zhu, A. Ma, et al. 2018. ABIN-1 regulates RIPK1 activation by linking Met1 ubiquitylation with Lys63 deubiquitylation in TNF-RSC. *Nat. Cell Biol.* 20:58–68. <https://doi.org/10.1038/s41556-017-0003-1>

el Marjou, F., K.P. Janssen, B.H. Chang, M. Li, V. Hindie, L. Chan, D. Louvard, P. Chambon, D. Metzger, and S. Robine. 2004. Tissue-specific and inducible Cre-mediated recombination in the gut epithelium. *Genesis.* 39:186–193.

Feoktistova, M., P. Geserick, B. Kellert, D.P. Dimitrova, C. Langlais, M. Hupe, K. Cain, M. MacFarlane, G. Häcker, and M. Leverkus. 2011. cIAPs block Ripoptosome formation, a RIP1/caspase-8 containing intracellular cell death complex differentially regulated by cFLIP isoforms. *Mol. Cell.* 43:449–463. <https://doi.org/10.1016/j.molcel.2011.06.011>

G'Sell, R.T., P.M. Gaffney, and D.W. Powell. 2015. A20-binding inhibitor of NF- κ B activation 1 is a physiologic inhibitor of NF- κ B: A molecular switch for inflammation and autoimmunity. *Arthritis Rheumatol.* 67:2292–2302. <https://doi.org/10.1002/art.39245>

Günther, C., E. Martini, N. Wittkopf, K. Amann, B. Weigmann, H. Neumann, M.J. Waldner, S.M. Hedrick, S. Tenzer, M.F. Neurath, and C. Becker. 2011. Caspase-8 regulates TNF- α -induced epithelial necroptosis and terminal ileitis. *Nature.* 477:335–339. <https://doi.org/10.1038/nature10400>

Günther, C., B. Buchen, G.-W. He, M. Hornef, N. Torow, H. Neumann, N. Wittkopf, E. Martini, M. Basic, A. Bleich, et al. 2015. Caspase-8 controls the gut response to microbial challenges by Tnf- α -dependent and independent pathways. *Gut.* 64:601–610. <https://doi.org/10.1136/gutjnl-2014-307226>

Heyninck, K., D. De Valck, W. Vanden Berghe, W. Van Crielinge, R. Contreras, W. Fiers, G. Haegeman, and R. Beyaert. 1999. The zinc finger protein A20 inhibits TNF-induced NF- κ B-dependent gene expression by interfering with an RIP- or TRAF2-mediated transactivation signal and directly

- binds to a novel NF- κ B-inhibiting protein ABIN. *J. Cell Biol.* 145:1471-1482. <https://doi.org/10.1083/jcb.145.7.1471>
- Hooper, L.V. 2015. Epithelial cell contributions to intestinal immunity. *Adv. Immunol.* 126:129-172. <https://doi.org/10.1016/bs.ai.2014.11.003>
- Jin, Z., Y. Li, R. Pitti, D. Lawrence, V.C. Pham, J.R. Lill, and A. Ashkenazi. 2009. Cullin3-based polyubiquitination and p62-dependent aggregation of caspase-8 mediate extrinsic apoptosis signaling. *Cell.* 137:721-735. <https://doi.org/10.1016/j.cell.2009.03.015>
- Justins, L., S. Ripke, R.K. Weersma, R.H. Duerr, D.P. McGovern, K.Y. Hui, J.C. Lee, L.P. Schumm, Y. Sharma, C.A. Anderson, et al.; International IBD Genetics Consortium (IIBDGC). 2012. Host-microbe interactions have shaped the genetic architecture of inflammatory bowel disease. *Nature.* 491:119-124. <https://doi.org/10.1038/nature11582>
- Justus, S.J., and A.T. Ting. 2015. Cloaked in ubiquitin, a killer hides in plain sight: The molecular regulation of RIPK1. *Immunol. Rev.* 266:145-160. <https://doi.org/10.1111/imr.12304>
- Kondylis, V., S. Kumari, K. Vlantis, and M. Pasparakis. 2017. The interplay of IKK, NF- κ B and RIPK1 signaling in the regulation of cell death, tissue homeostasis and inflammation. *Immunol. Rev.* 277:113-127. <https://doi.org/10.1111/imr.12550>
- Lee, E.G., D.L. Boone, S. Chai, S.L. Libby, M. Chien, J.P. Lodolce, and A. Ma. 2000. Failure to regulate TNF-induced NF- κ B and cell death responses in A20-deficient mice. *Science.* 289:2350-2354. <https://doi.org/10.1126/science.289.5488.2350>
- Lu, T.T., M. Onizawa, G.E. Hammer, E.E. Turer, Q. Yin, E. Damko, A. Agelidis, N. Shifrin, R. Advincula, J. Barrera, et al. 2013. Dimerization and ubiquitin mediated recruitment of A20, a complex deubiquitinating enzyme. *Immunity.* 38:896-905. <https://doi.org/10.1016/j.immuni.2013.03.008>
- Ma, A., and B.A. Malynn. 2012. A20: Linking a complex regulator of ubiquitylation to immunity and human disease. *Nat. Rev. Immunol.* 12:774-785. <https://doi.org/10.1038/nri3313>
- Majumdar, I., V. Ahuja, and J. Paul. 2017. Altered expression of tumor necrosis factor alpha-induced protein 3 correlates with disease severity in ulcerative colitis. *Sci. Rep.* 7:9420. <https://doi.org/10.1038/s41598-017-09796-9>
- Matsuzawa, Y., S. Oshima, M. Takahara, C. Maeyashiki, Y. Nemoto, M. Kobayashi, Y. Nibe, K. Nozaki, T. Nagaishi, R. Okamoto, et al. 2015. TNF AIP3 promotes survival of CD4 T cells by restricting MTOR and promoting autophagy. *Autophagy.* 11:1052-1062. <https://doi.org/10.1080/15548627.2015.1055439>
- Matsuzawa-Ishimoto, Y., Y. Shono, L.E. Gomez, V.M. Hubbard-Lucey, M. Cammer, J. Neil, M.Z. Dewan, S.R. Lieberman, A. Lazrak, J.M. Marinis, et al. 2017. Autophagy protein ATG16L1 prevents necroptosis in the intestinal epithelium. *J. Exp. Med.* 214:3687-3705. <https://doi.org/10.1084/jem.20170558>
- Nanda, S.K., R.K.C. Venigalla, A. Ordureau, J.C. Patterson-Kane, D.W. Powell, R. Toth, J.S.C. Arthur, and P. Cohen. 2011. Polyubiquitin binding to ABIN1 is required to prevent autoimmunity. *J. Exp. Med.* 208:1215-1228. <https://doi.org/10.1084/jem.20102177>
- Newton, K., K.E. Wickliffe, A. Maltzman, D.L. Dugger, A. Strasser, V.C. Pham, J.R. Lill, M. Roose-Girma, S. Warming, M. Solon, et al. 2016. RIPK1 inhibits ZBP1-driven necroptosis during development. *Nature.* 540:129-133. <https://doi.org/10.1038/nature20559>
- Onizawa, M., S. Oshima, U. Schulze-Topphoff, J.A. Osés-Prieto, T. Lu, R. Tavares, T. Prodhomme, B. Duong, M.I. Whang, R. Advincula, et al. 2015. The ubiquitin-modifying enzyme A20 restricts ubiquitination of the kinase RIPK3 and protects cells from necroptosis. *Nat. Immunol.* 16:618-627. <https://doi.org/10.1038/ni.3172>
- Pipari, A.W. Jr., M.S. Boguski, and V.M. Dixit. 1990. The A20 cDNA induced by tumor necrosis factor alpha encodes a novel type of zinc finger protein. *J. Biol. Chem.* 265:14705-14708.
- Oshima, S., E.E. Turer, J.A. Callahan, S. Chai, R. Advincula, J. Barrera, N. Shifrin, B. Lee, T.S. Benedict Yen, T. Woo, et al. 2009. ABIN-1 is a ubiquitin sensor that restricts cell death and sustains embryonic development. *Nature.* 457:906-909. <https://doi.org/10.1038/nature07575>
- Sato, T., and H. Clevers. 2012. Primary mouse small intestinal epithelial cell cultures. In *Epithelial Cell Culture Protocols*. S.H. Randell, and M.L. Fulcher, editors. Humana Press, Totowa, NJ. 319-328. https://doi.org/10.1007/978-1-62703-125-7_19
- Schuijjs, M.J., M.A. Willart, K. Vergote, D. Gras, K. Deswarte, M.J. Ege, F.B. Madeira, R. Beyaert, G. van Loo, F. Bracher, et al. 2015. Farm dust and endotoxin protect against allergy through A20 induction in lung epithelial cells. *Science.* 349:1106-1110. <https://doi.org/10.1126/science.aac6623>
- Shao, L., S. Oshima, B. Duong, R. Advincula, J. Barrera, B.A. Malynn, and A. Ma. 2013. A20 restricts wnt signaling in intestinal epithelial cells and suppresses colon carcinogenesis. *PLoS One.* 8:e62223-e62227. <https://doi.org/10.1371/journal.pone.0062223>
- Skaug, B., J. Chen, F. Du, J. He, A. Ma, and Z.J. Chen. 2011. Direct, noncatalytic mechanism of IKK inhibition by A20. *Mol. Cell.* 44:559-571. <https://doi.org/10.1016/j.molcel.2011.09.015>
- Takahashi, N., L. Duprez, S. Grootjans, A. Cauwels, W. Nerinckx, J.B. DuHadaway, V. Goossens, R. Roelandt, F. Van Hauwermeiren, C. Libert, et al. 2012. Necrostatin-1 analogues: Critical issues on the specificity, activity and in vivo use in experimental disease models. *Cell Death Dis.* 3:e437. <https://doi.org/10.1038/cddis.2012.176>
- Takahashi, N., L. Vereecke, M.J.M. Bertrand, L. Duprez, S.B. Berger, T. Divert, A. Gonçalves, M. Sze, B. Gilbert, S. Kourula, et al. 2014. RIPK1 ensures intestinal homeostasis by protecting the epithelium against apoptosis. *Nature.* 513:95-99. <https://doi.org/10.1038/nature13706>
- Tavares, R.M., E.E. Turer, C.L. Liu, R. Advincula, P. Scapini, L. Rhee, J. Barrera, C.A. Lowell, P.J. Utz, B.A. Malynn, and A. Ma. 2010. The ubiquitin modifying enzyme A20 restricts B cell survival and prevents autoimmunity. *Immunity.* 33:181-191. <https://doi.org/10.1016/j.immuni.2010.07.017>
- Tenev, T., K. Bianchi, M. Darding, M. Broemer, C. Langlais, F. Wallberg, A. Zachariou, J. Lopez, M. MacFarlane, K. Cain, and P. Meier. 2011. The Ripoptosome, a signaling platform that assembles in response to genotoxic stress and loss of IAPs. *Mol. Cell.* 43:432-448. <https://doi.org/10.1016/j.molcel.2011.06.006>
- Tokunaga, F., H. Nishimasu, R. Ishitani, E. Goto, T. Noguchi, K. Mio, K. Kamei, A. Ma, K. Iwai, and O. Nureki. 2012. Specific recognition of linear polyubiquitin by A20 zinc finger 7 is involved in NF- κ B regulation. *EMBO J.* 31:3856-3870. <https://doi.org/10.1038/emboj.2012.241>
- van Deen, W.K., M.G.H. van Oijen, K.D. Myers, A. Centeno, W. Howard, J.M. Choi, B.E. Roth, E.M. McLaughlin, D. Hollander, B. Wong-Swanson, et al. 2014. A nationwide 2010-2012 analysis of U.S. health care utilization in inflammatory bowel diseases. *Inflamm. Bowel Dis.* 20:1747-1753. <https://doi.org/10.1097/MIB.0000000000000139>
- Vereecke, L., M. Sze, C. Mc Guire, B. Rogiers, Y. Chu, M. Schmidt-Supprian, M. Pasparakis, R. Beyaert, and G. van Loo. 2010. Enterocyte-specific A20 deficiency sensitizes to tumor necrosis factor-induced toxicity and experimental colitis. *J. Exp. Med.* 207:1513-1523. <https://doi.org/10.1084/jem.20092474>
- Vereecke, L., S. Vieira-Silva, T. Billiet, J.H. van Es, C. Mc Guire, K. Slowicka, M. Sze, M. van den Born, G. De Hertogh, H. Clevers, et al. 2014. A20 controls intestinal homeostasis through cell-specific activities. *Nat. Commun.* 5:5103.
- Verhelst, K., I. Carpentier, M. Kreike, L. Meloni, L. Verstrepen, T. Kensche, I. Dikic, and R. Beyaert. 2012. A20 inhibits LUBAC-mediated NF- κ B activation by binding linear polyubiquitin chains via its zinc finger 7. *EMBO J.* 31:3845-3855. <https://doi.org/10.1038/emboj.2012.240>
- Verstrepen, L., I. Carpentier, and R. Beyaert. 2014. The biology of A20-binding inhibitors of NF- κ B activation (ABINs). *Adv. Exp. Med. Biol.* 809:13-31. https://doi.org/10.1007/978-1-4939-0398-6_2
- Vlantis, K., A. Wullaert, A. Polykratis, V. Kondylis, M. Dannappel, R. Schwarzer, P. Welz, T. Corona, H. Walczak, F. Weih, et al. 2016. NEMO prevents RIP kinase 1-mediated epithelial cell death and chronic intestinal inflammation by NF- κ B-dependent and -independent functions. *Immunity.* 44:553-567. <https://doi.org/10.1016/j.immuni.2016.02.020>
- Wagner, S., I. Carpentier, V. Rogov, M. Kreike, F. Ikeda, F. Löhr, C.-J. Wu, J.D. Ashwell, V. Dötsch, I. Dikic, and R. Beyaert. 2008. Ubiquitin binding mediates the NF- κ B inhibitory potential of ABIN proteins. *Oncogene.* 27:3739-3745. <https://doi.org/10.1038/sj.onc.1211042>
- Wang, L., F. Du, and X. Wang. 2008. TNF- α induces two distinct caspase-8 activation pathways. *Cell.* 133:693-703. <https://doi.org/10.1016/j.cell.2008.03.036>
- Wang, S., F. Wen, G.B. Wiley, M.T. Kinter, and P.M. Gaffney. 2013. An enhancer element harboring variants associated with systemic lupus erythematosus engages the TNFAIP3 promoter to influence A20 expression. *PLoS Genet.* 9:e1003750. <https://doi.org/10.1371/journal.pgen.1003750>
- Weisel, K., N.E. Scott, D.J. Tompson, B.J. Votta, S. Madhavan, K. Povey, A. Wolstenholme, M. Simeoni, T. Rudo, L. Richards-Peterson, et al. 2017. Randomized clinical study of safety, pharmacokinetics, and pharmacodynamics of RIPK1 inhibitor GSK2982772 in healthy volunteers. *Pharmacol. Res. Perspect.* 5:e00365. <https://doi.org/10.1002/prp2.365>
- Wertz, I., and V. Dixit. 2014. A20--a bipartite ubiquitin editing enzyme with immunoregulatory potential. *Adv. Exp. Med. Biol.* 809:1-12.
- Wertz, I.E., K.M. O'Rourke, H. Zhou, M. Eby, L. Aravind, S. Seshagiri, P. Wu, C. Wiesmann, R. Baker, D.L. Boone, et al. 2004. De-ubiquitination and

- ubiquitin ligase domains of A20 downregulate NF- κ B signalling. *Nature*. 430:694–699. <https://doi.org/10.1038/nature02794>
- Wertz, I.E., K. Newton, D. Seshasayee, S. Kusam, C. Lam, J. Zhang, N. Popovych, E. Helgason, A. Schoeffler, S. Jeet, et al. 2015. Phosphorylation and linear ubiquitin direct A20 inhibition of inflammation. *Nature*. 528:370–375. <https://doi.org/10.1038/nature16165>
- Wlodarska, M., A.D. Kostic, and R.J. Xavier. 2015. An integrative view of microbiome-host interactions in inflammatory bowel diseases. *Cell Host Microbe*. 17:577–591. <https://doi.org/10.1016/j.chom.2015.04.008>
- Yamaguchi, N., and N. Yamaguchi. 2015. The seventh zinc finger motif of A20 is required for the suppression of TNF- α -induced apoptosis. *FEBS Lett*. 589:1369–1375. <https://doi.org/10.1016/j.febslet.2015.04.022>
- Zeissig, S., C. Bojarski, N. Buergel, J. Mankertz, M. Zeitz, M. Fromm, and J.D. Schulzke. 2004. Downregulation of epithelial apoptosis and barrier repair in active Crohn's disease by tumour necrosis factor alpha antibody treatment. *Gut*. 53:1295–1302. <https://doi.org/10.1136/gut.2003.036632>
- Zhou, Q., H. Wang, D.M. Schwartz, M. Stoffels, Y.H. Park, Y. Zhang, D. Yang, E. Demirkaya, M. Takeuchi, W.L. Tsai, et al. 2016. Loss-of-function mutations in TNFAIP3 leading to A20 haploinsufficiency cause an early-onset autoinflammatory disease. *Nat. Genet*. 48:67–73. <https://doi.org/10.1038/ng.3459>